Research Square

Preprints are preliminary reports that have not undergone peer review.
They should not be considered conclusive, used to inform clinical practice,
or referenced by the media as validated information.

A regulatory closed loop between serotonergic signaling and sensory processing

Tansu Celikel

celikel@gatech.edu

Georgia Institute of Technology

Tousif Jamal

Social Brain Lab, Netherlands Institute for Neuroscience

Xuan Yan

Center for Excellence in Brain Science and Intelligence Technology

Mehmet Ali Deveci

Kari Bosch

Judith Homberg

Radboud University Medical center https://orcid.org/0000-0002-7621-1010

Article

Keywords:

Posted Date: November 13th, 2026

DOI: https://doi.org/10.21203/rs.3.rs-11466669/v1

License: This work is licensed under a Creative Commons Attribution 4.0 International License.
Read Full License

Additional Declarations: There is **NO** Competing Interest.

A regulatory closed loop between serotonergic signaling and sensory processing

Tousif Jamal[1,2], Xuan Yan[1], Mehmet Ali Deveci[1], Kari Bosch[3], Judith R. Homberg[1,3], and Tansu Celikel[1,4,5]

[1] *Donders Institute for Brain, Cognition and Behaviour, Radboud University, Heyendaalseweg 135, 6525 AJ Nijmegen, The Netherlands*

[2] *Social Brain Lab, Netherlands Institute for Neuroscience, Meibergdreef 47, 1105 BA Amsterdam, The Netherlands*

[3] *Department of Medical Neuroscience, Radboud University Medical Center, Geert Grooteplein Zuid 10, 6525 GA Nijmegen, The Netherlands*

[4] *School of Psychological and Brain Sciences, Georgia Institute of Technology, 654 Cherry Street, Atlanta, GA 30332, USA*

[5] *Georgia Tech-CNRS IRL 2958, Georgia Tech-Europe, 2 Rue Marconi, 57070 Metz, France*

Correspondence: Tansu Celikel (celikel@gatech.edu)

ABSTRACT

Serotonin (5-HT) shapes sensory, cognitive and emotional functions, partly by regulating the excitation–inhibition balance of neural circuits. Whether sensory experience in turn regulates cortical serotonergic signaling is unknown. Here we combine column- and layer-resolved transcriptomics of the juvenile mouse barrel cortex with network analysis and whole-cell recordings. Two weeks of whisker deprivation suppresses transcription of genes governing 5-HT metabolism, reuptake and release. These changes are layer-specific, extend to neighboring columns and reverse two columns away, where serotonin receptor transcripts are upregulated. Network analysis identifies experience-dependent hub genes, including *Spr*, *Snca* and *Maoa*, that couple serotonergic and dopaminergic pathways. Activation of 5-HT1F, a receptor whose gene *Htr1f* is differentially transcribed across the deprived barrel field, reduces excitability of layer 2/3 pyramidal neurons by depolarizing the spike threshold. Sensory experience thus shapes the cortical serotonergic transcriptome, which in turn controls neuronal excitability, suggesting a regulatory closed loop between sensory processing and neuromodulation.

INTRODUCTION

Serotonin (5-hydroxytryptamine; 5-HT) is an evolutionarily conserved monoaminergic neuromodulator implicated in mood, learning and memory, cognition, reward behavior, and circadian rhythm regulation[1–3]. In the developing barrel cortex, which represents the whiskers in rodents, 5-HT plays especially prominent roles. The serotonin transporter (SERT) is transiently expressed in non-serotonergic thalamocortical neurons, prenatally from embryonic day 15.5, before 5-HTergic fibers reach the cortex (S. Samina et al., unpublished data), and postnatally until the second postnatal week[4–6]. There, SERT prevents overactivation of presynaptic 5-HT1B receptors on thalamocortical afferents (TCAs), thereby protecting layer 4 (L4) from glutamate-induced neurotoxicity and enabling proper barrel formation[7–9]. Conversely, elevated extracellular 5-HT during this critical window, caused by genetic loss of SERT or by perinatal exposure to selective serotonin reuptake inhibitors (SSRIs), disrupts both the topological organization of TCAs and the formation of L4 excitatory circuits[9,10], and alters somatosensory processing and whisker-based behavior[11–16].

During development, the 5-HT system does not mature in isolation but interacts with the dopaminergic system[1,17]. Prenatal absence of tryptophan hydroxylase 2, the rate-limiting enzyme for 5-HT synthesis, not only reduces 5-HT fiber density but also causes local hyperinnervation of the prefrontal cortex by dopaminergic fibers, and embryos lacking SERT show a similar trend together with upregulation of monoamine oxidase A (*Maoa*), which degrades both 5-HT and dopamine (S. Samina et al., unpublished data). In the early postnatal brain, the absence of SERT is associated with changes in both serotonergic and dopaminergic projections to the prefrontal cortex[18]. Such serotonin–dopamine interactions plausibly extend to the barrel cortex, where we recently showed that sensory experience regulates the dopaminergic signaling pathway (DSP)[19].

In the adult barrel cortex, serotonergic innervation from the dorsal raphe nucleus (DRN) is topographically organized and layer-, region-, and cell-type specific[20–22], neuromodulatory nuclei project to multiple stages of the whisker system[23], and electrical stimulation of the DRN enhances the whisker-evoked responses of barrel cortex neurons[17,24]. Fluorescent 5-HT biosensors now reveal sensory-evoked serotonin release in the neocortex in vivo[25]. Conversely, sensory experience regulates serotonergic signaling: visual deprivation alters 5-HT levels in the visual system[26], and 5-HT mediates cross-modal reorganization of cortical circuits after sensory loss[27,28]. Yet whether sensory experience systematically regulates serotonergic gene expression in the cortex, and what functional consequences such regulation might have, remains unknown.

The barrel cortex is a well-characterized sensory model system in which each cortical column represents a single whisker, providing exceptional anatomical precision for studying experience-dependent plasticity[29–33]. Whisker deprivation after the first postnatal week potently reorganizes barrel cortex circuits through both Hebbian and homeostatic mechanisms[34–40], at the level of synapses, cells, axonal arbors and population activity[41–45]. Leveraging a columnar and laminar transcriptomic dataset of the barrel cortex[46], we asked whether sensory deprivation regulates the transcription of the 157 genes constituting the serotonergic signaling pathway (SSP). We combined differential expression analysis with mutual-information-based network analysis to identify transcriptional hubs, compared the reorganized SSP with the DSP, and tested the function of the 5-HT1F receptor, encoded by the experience-dependent transcript *Htr1f*, with whole-cell recordings. We show that whisker deprivation suppresses serotonergic transcription in a layer- and column-specific manner, reorganizes serotonergic and dopaminergic co-expression networks around shared hub genes, and that 5-HT1F activation reduces the excitability of L2/3

pyramidal neurons. These results suggest a regulatory closed loop between sensory experience and serotonergic neuromodulation in the developing somatosensory cortex.

RESULTS

Serotonergic transcription is laminar-uniform at baseline

We identified 157 genes involved in serotonin metabolism, reuptake, release and receptor signaling using gene ontology annotation (Fig. 1A–C). In control animals (no whisker deprivation), the overall distribution of serotonergic transcript counts did not differ significantly between the granular layer (L4) and supragranular layers (L2/3; $P = 0.11$, Kolmogorov–Smirnov test; Fig. 1D). Pairwise comparison of individual gene transcription across layers confirmed the absence of laminar bias (adjusted $R^2 = 0.90$, $P = 0.59$, t-test; Fig. 1E). Functional gene subgroups covering serotonin receptor signaling, metabolism, uptake and release similarly showed no significant laminar differences ($0.10 < P < 0.88$, t-test; Fig. 1F). In situ hybridization data from the Allen Mouse Brain Atlas independently confirmed these laminar profiles for a subset of genes (Supplementary Fig. 1). These results are consistent with the diffuse axonal projections of DRN neurons into the developing somatosensory cortex[17,47], and suggest that serotonergic signaling in the juvenile barrel cortex is not intrinsically laminar-specific.

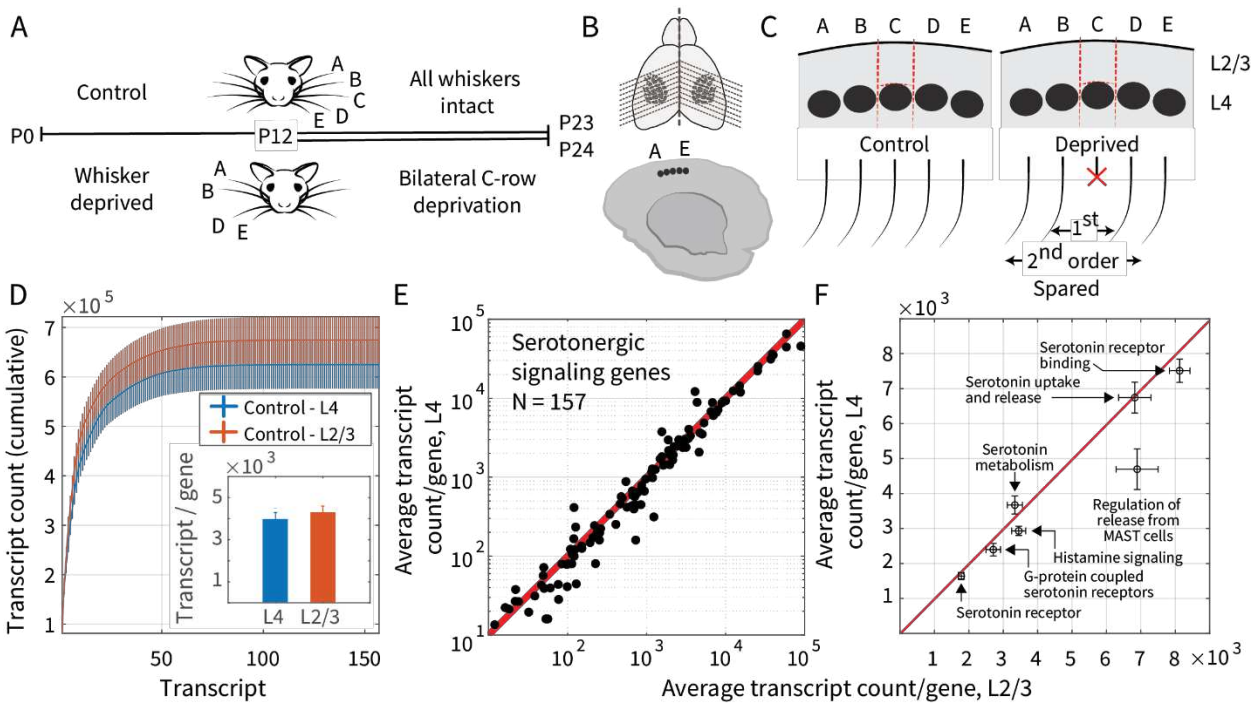


Figure 1: Serotonergic gene transcription is laminar-uniform in the juvenile barrel cortex.

A. Sensory deprivation protocol (N = 4 mice per group).

B. Preparation of thalamocortical slices from the barrel cortex.

C. Isolation of cortical columns and specific laminar regions, followed by RNA sequencing[46,71]. Cartoons in panels A–C are adapted, with permission.

D. Serotonergic signaling genes identified by gene ontology analysis show comparable transcription across the granular layer (L4) and supragranular layers (L2/3) (P = 0.11, Kolmogorov–Smirnov test). The inset shows the average transcript counts per lamina (N = 157 genes).

E. Pairwise comparison of gene transcription across layers; each dot represents an individual gene. No significant differences in transcription were observed across layers (linear regression, adjusted $R^2 = 0.90$, P = 0.59, t-test).

F. Functional categorization of genes showed no significant differences in transcription across laminae within gene clusters ($0.10 < P < 0.88$, t-test).

RNA-seq data, including read alignments (BAM files) and raw read counts generated with the STAR aligner, are publicly available[74]. Data acquisition, processing, quality control and validation have been reported[46].

Whisker deprivation suppresses serotonergic transcription

Two weeks of bilateral C-row whisker plucking, a protocol that induces robust synaptic and cellular plasticity in the barrel cortex[34–37], suppressed serotonergic gene transcription in both L4

125 ($P < 0.05$, Kolmogorov–Smirnov test; $F(1,156) = 14.70$, $P < 0.001$, ANOVA; Fig. 2A) and L2/3
126 ($P < 0.05$, Kolmogorov–Smirnov test; $F(1,156) = 9.15$, $P < 0.01$, ANOVA; Fig. 2B). Most
127 transcripts were downregulated in both layers, with deprived/control ratios clustering below
128 unity (Fig. 2C). Affected genes spanned multiple functional classes: serotonin release and
129 synaptic transmission (L2/3: $P < 0.01$; L4: $P = 0.01$), serotonergic neuron development (both
130 layers: $P < 0.005$), serotonin metabolism (both layers: $P < 0.001$), G-protein-dependent signal
131 transduction (L2/3: $P < 0.01$; L4: $P < 0.001$), and serotonin receptor binding (both layers: $P <$
132 0.005; all comparisons: t-test with Storey false discovery rate correction; Fig. 2D,E).

133 Only two transcripts were selectively regulated in L4: *Oaz3*, which encodes an ornithine
134 decarboxylase antizyme that inhibits polyamine uptake, and *Htr1b*, which encodes the 5-HT1B
135 receptor implicated in thalamocortical development[7,9]. In contrast, L2/3 showed a broader set of
136 experience-regulated transcripts spanning serotonin metabolism, receptor expression and mast
137 cell-mediated release (Fig. 2D,E), raising the possibility that local, non-neuronal sources of 5-HT
138 are also under sensory control.

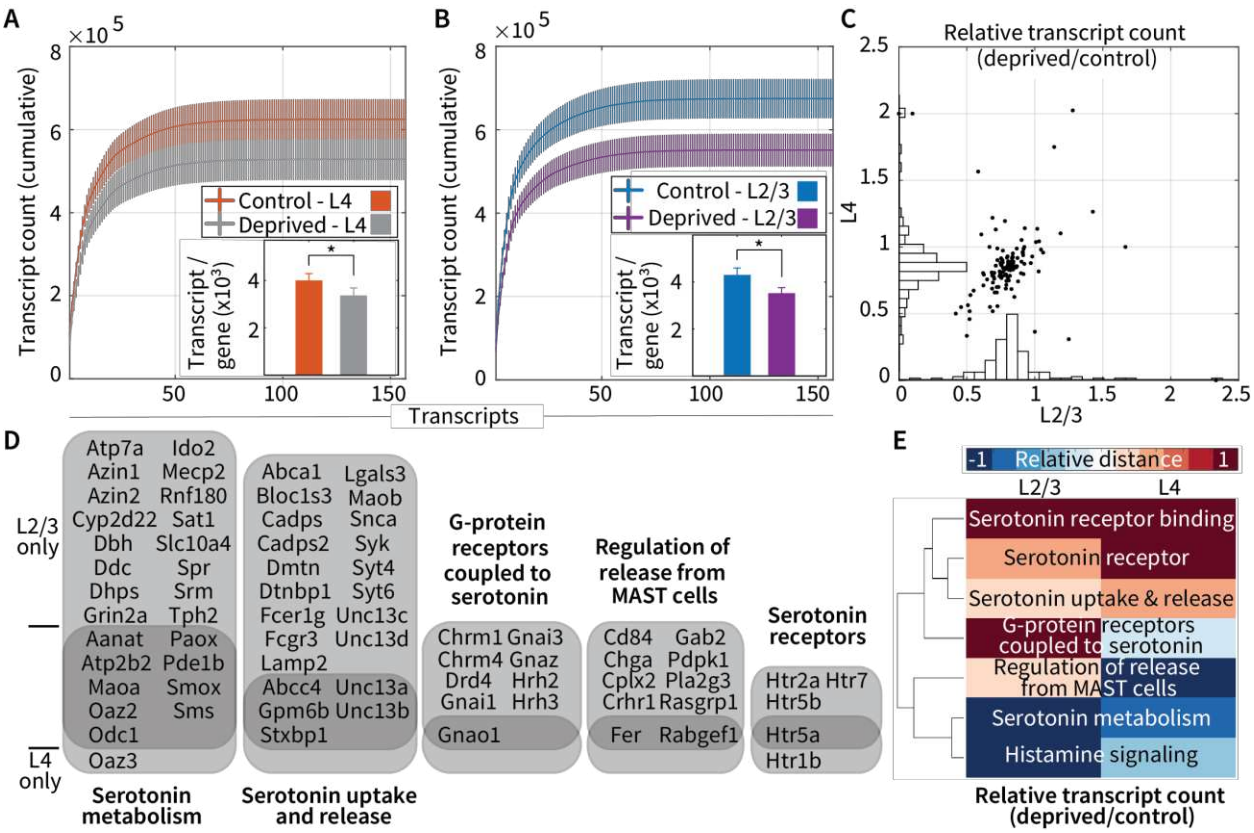


Figure 2: Whisker deprivation suppresses the serotonergic transcriptome.

A. Whisker deprivation suppresses gene transcription in L4 of the C column in juvenile mice; sham-deprived (Control) versus whisker-deprived (Deprived) animals ($P < 0.05$, Kolmogorov–Smirnov test). Inset: average number of transcripts per gene across conditions ($F(1,156) = 14.70$, $P < 0.001$; ANOVA).

B. Whisker deprivation suppresses serotonergic gene transcription in L2/3 ($P < 0.05$, Kolmogorov–Smirnov test). Inset: average transcript count ($F(1,156) = 9.15$, $P < 0.01$; ANOVA).

C. Relative transcript count (deprived/control) of each gene in L2/3 versus L4; marginal histograms show the distributions.

D. Serotonergic transcripts whose transcription is altered upon whisker deprivation are grouped by simplified functional annotations. Note that the intersection of the two rounded rectangles, shaded in dark grey, contains transcripts that are regulated by whisker deprivation both in L2/3 and L4.

E. Clustergram of the relative distance between functional groups. Data were normalized within laminae across whisker deprivation conditions. Whisker deprivation significantly altered the transcription of genes responsible for serotonin release and synaptic transmission (L2/3: $P < 0.01$; L4: $P = 0.01$), serotonergic neuron development (L2/3: $P < 0.005$; L4: $P < 0.005$), serotonin metabolism (L2/3: $P < 0.001$; L4: $P < 0.001$), G-protein-dependent signal

transduction in the serotonergic pathway (L2/3: $P < 0.01$; L4: $P < 0.001$), and serotonin binding (L2/3: $P < 0.005$; L4: $P < 0.005$; all comparisons: t-test). All P values in all figures are corrected for multiple comparisons using the false discovery rate method[73].

Transcriptional changes spread to neighboring columns

Because DRN afferents project diffusely into the cortex, we asked whether experience-dependent serotonergic changes are confined to the deprived column or propagate across the barrel field. The deprived C column and its first-order neighbors (B/D columns, whose principal whiskers remained intact) had statistically indistinguishable serotonergic transcriptional profiles in both L4 ($P = 0.99$, Kolmogorov–Smirnov test; $F(1,156) = 0.31$, $P = 1.0$, ANOVA) and L2/3 ($P = 0.53$, Kolmogorov–Smirnov test; $F(1,156) = 0.64$, $P = 0.99$, ANOVA; Fig. 3A–C), across all functional gene classes (Fig. 3D–F; FDR adjusted values). Thus, intact ascending sensory input to neighboring columns does not locally compensate for deprivation-induced transcriptional changes.

In contrast, the A/E columns (second-order neighbors, two columns away from the deprived C column) showed significantly higher serotonergic transcription than the deprived column in both L4 ($F(1,156) = 18.93$, $P < 0.001$) and L2/3 ($F(1,156) = 20.48$, $P < 0.001$; Fig. 4A–C), restoring transcript levels to those of control animals (Fig. 4C). This upregulation was enriched in serotonin receptor transcripts, including *Htr1f*, and was not laminar-specific (Fig. 4D,E), in contrast to the L2/3-dominant suppression in the deprived column. Deprivation-induced transcriptional changes therefore spread across the barrel field, with receptor upregulation at the periphery of the deprived region.

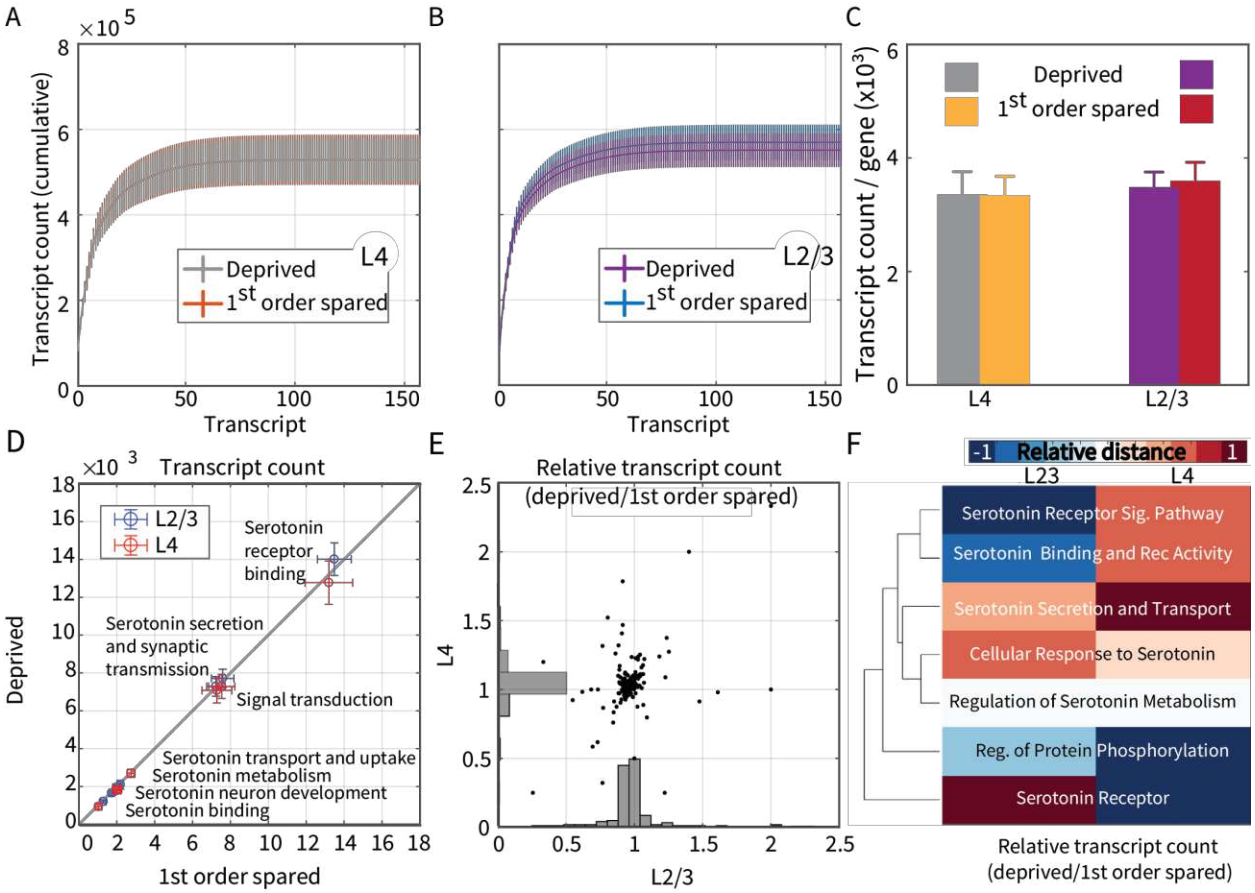


Figure 3: After sensory deprivation, the serotonergic transcriptome is comparable across the deprived and first-order neighboring columns. The principal whiskers of first-order neighboring columns were intact throughout the experiment.

A. Cumulative transcript count in L4 ($P = 0.99$; two-sample Kolmogorov–Smirnov test).

B. Cumulative transcript count in L2/3 ($P = 0.53$; two-sample Kolmogorov–Smirnov test).

C. Average transcript count per gene. L4: $F(1,156) = 0.31$, $P = 1$; L2/3: $F(1,156) = 0.64$, $P = 0.99$. All comparisons are within animals across columns; none is statistically significant.

D. Mean transcript count per functional gene class in the deprived column versus first-order spared columns, for L2/3 (blue) and L4 (red); the diagonal marks equality.

E. Relative transcript count (deprived/first-order spared) of each gene in L2/3 versus L4; marginal histograms show the distributions.

F. Clustergram of the relative distance between functional gene classes, normalized within laminae across columns.

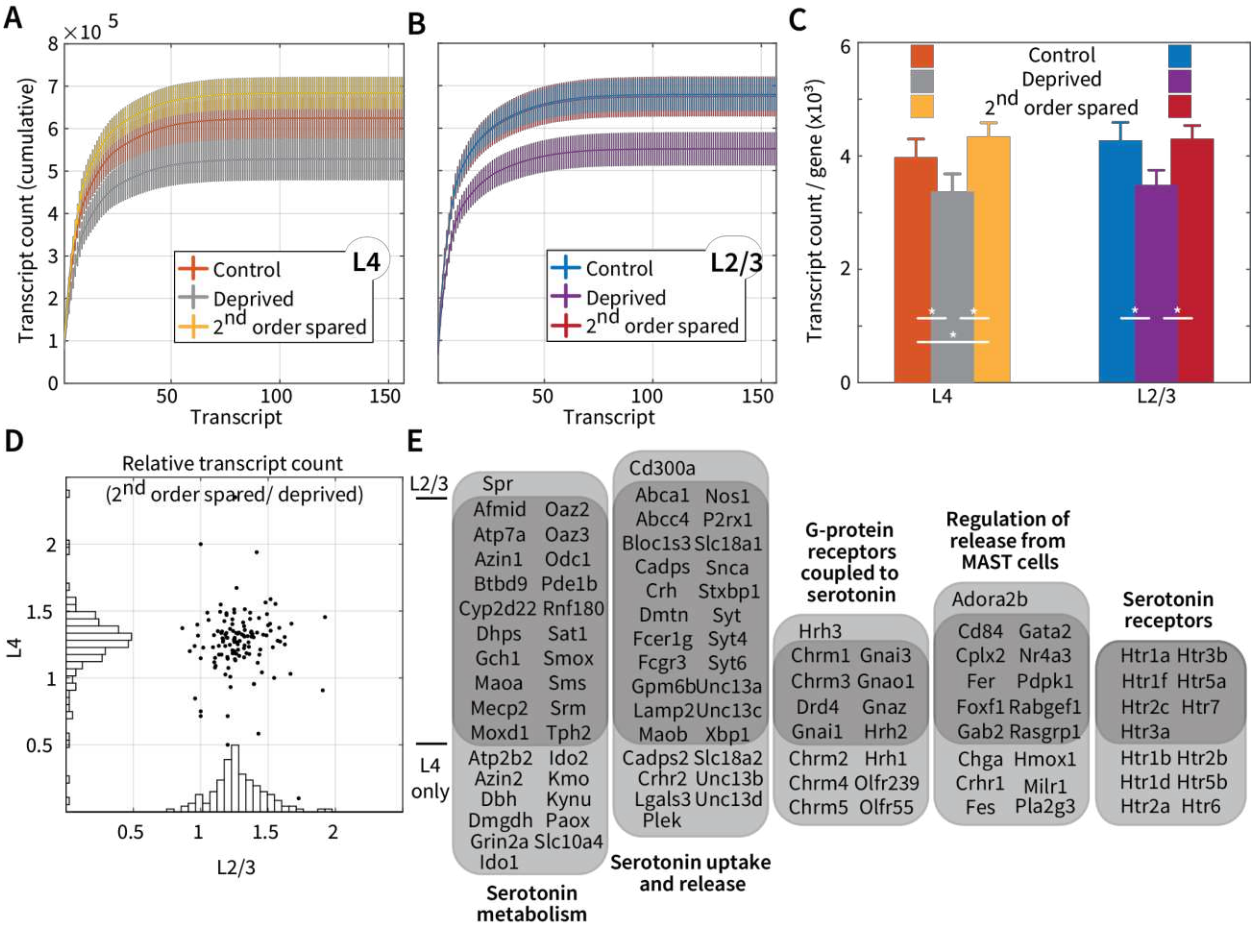


Figure 4: **Topography of experience-dependent changes in serotonergic gene transcription. Second-order neighboring columns (A/E) are compared with the deprived C column in deprived animals.**

A, B. Transcription of serotonergic signaling genes is potentiated two columns away from the deprived column in L4 (A) and L2/3 (B) ($P < 0.05$, Kolmogorov–Smirnov test).

C. Average transcript count per gene across sensory experience conditions and laminae; statistically significant comparisons are shown. Within-animal comparisons across columns used the paired t-test; between-animal comparisons used ANOVA (L4: $F(1,156) = 18.93$, $P < 0.001$; L2/3: $F(1,156) = 20.48$, $P < 0.001$).

D. Relative transcript count (second-order spared/deprived) of each gene in L2/3 versus L4; marginal histograms show the distributions.

E. Serotonergic transcripts whose transcription differs between the deprived column and second-order neighboring columns, grouped by simplified functional annotation. The intersection of the two rounded rectangles contains transcripts regulated in both L2/3 and L4.

5-HT1F activation reduces L2/3 neuronal excitability

Among the experience-regulated receptor transcripts, *Htr1f*, which encodes the 5-HT1F receptor, differed between the deprived column and second-order spared columns in both L2/3 and L4 (Fig. 4E). 5-HT1F is a Gi/o-coupled receptor that inhibits adenylyl cyclase[48], but its role in cortical neurons is poorly understood. To determine how 5-HT1F signaling affects cortical excitability, we analyzed whole-cell current-clamp recordings from L2/3 pyramidal neurons in acute barrel cortex slices of adult, non-deprived mice[49]. Bath application of the 5-HT1F agonist LY334370 (5 μM)[50] consistently reduced the number of action potentials (APs) evoked by somatic depolarization (Fig. 5A,B) and decreased firing rate at both maximal ($P < 0.001$) and half-maximal ($P < 0.02$) stimulus intensities (Fig. 5C). 5-HT1F activation also increased the latency to the first AP ($P < 0.001$; Fig. 5D) and narrowed the temporal window of spiking ($P < 0.005$; Fig. 5E). These effects are at least partly attributable to depolarization of the AP threshold ($P < 0.005$; Fig. 5F), which is expected to reduce firing rate and lengthen the inter-spike interval, as observed ($P < 0.05$; Fig. 5G). All comparisons used two-sided paired t-tests within cells ($N = 8$ neurons from 4 mice). Thus, 5-HT1F signaling limits the excitability of L2/3 pyramidal neurons in a cortical region where *Htr1f* transcription is regulated by sensory experience.

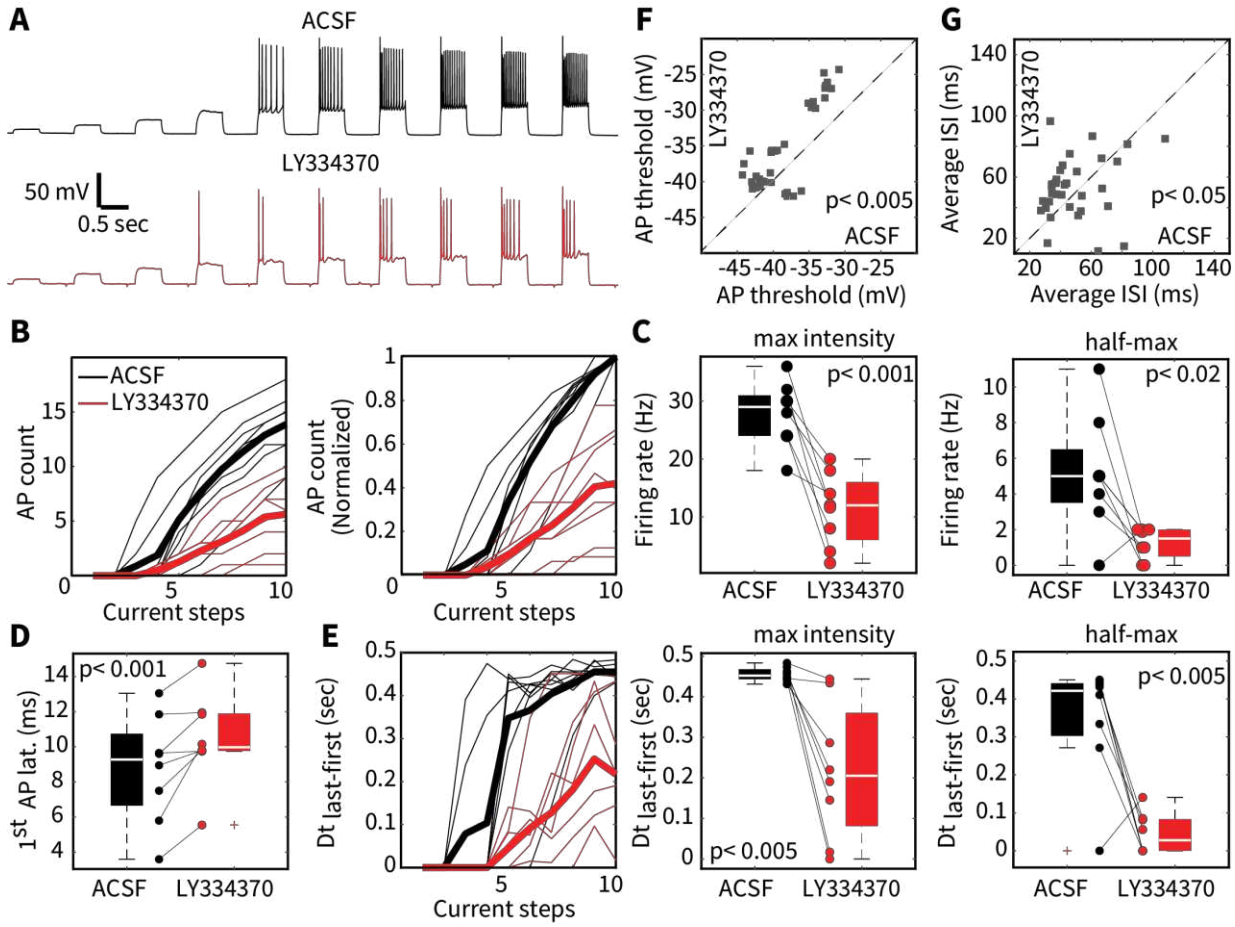


Figure 5: Activation of 5-HT1F suppresses the excitability of L2/3 pyramidal neurons.

A. Representative whole-cell current-clamp recordings from adult L2/3 pyramidal neurons in the barrel cortex under control (ACSF) conditions and during activation of 5-HT1F with LY334370 (5 μM). Somatic depolarization was applied as step-and-hold pulses (0.5 s per pulse; 40 pA per step; 10 steps).

B. Left: number of action potentials (APs) generated during somatic stimulation. Thin lines, individual neurons; thick lines, group averages. Right: AP count normalized to the count evoked by the maximum stimulus intensity under control conditions.

C. Firing rate at the maximum (left) and half-maximum (right) stimulus intensity.

D. Latency to first action potential at the maximum stimulus intensity.

E. Temporal window of spiking across stimulus intensities and conditions. The stimulus duration was 0.5 s.

F. Membrane voltage at which the first AP is triggered (AP threshold), ACSF versus LY334370.

G. Average inter-spike interval (ISI) before and during 5-HT1F activation. All statistical comparisons are two-sided paired t-tests (N = 8 neurons from 4 mice).

Deprivation reorganizes serotonergic co-expression networks

To characterize the network-level consequences of whisker deprivation, we applied mutual-information-based network analysis (NETSCOPE[51]) to the SSP transcriptome in L2/3 and L4 under control and deprived conditions (Fig. 6). In L2/3, whisker deprivation reduced connectivity among genes involved in histamine signaling and serotonin uptake and release, while genes in the serotonin metabolism and receptor binding clusters showed increased degree centrality. In L4, the pattern was partially reversed: connectivity among serotonin uptake and release genes increased, while G-protein-coupled receptor genes showed reduced connectivity in both layers. Connectivity of genes regulating mast cell release was more strongly suppressed in L4 than in L2/3, consistent with layer-specific neuroimmune modulation of serotonergic signaling. After deprivation, *Spr* and *Snca* became the most central nodes in L2/3, replacing *Maoa* and *Ddc* in control networks, whereas *Abcc4* and *Dtnbp1* dominated the deprived L4 network (Fig. 6). Hub genes, those with high betweenness centrality in the differential network, are candidate transcriptional drivers of experience-dependent serotonergic remodeling (Fig. 6; Supplementary Fig. 2). Because biological co-expression networks have non-random topologies that carry functional information[52], such hubs are unlikely to be incidental.

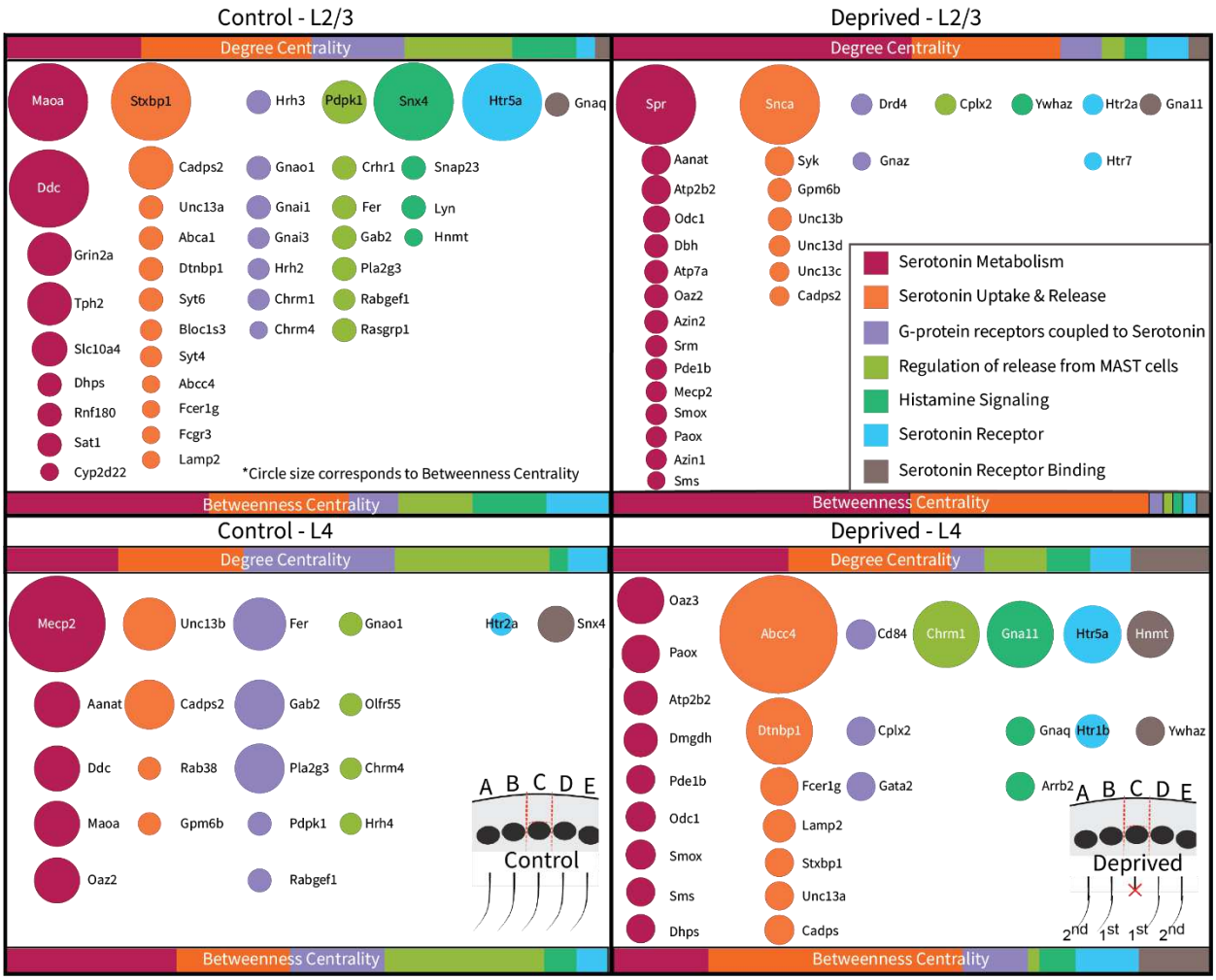


Figure 6: Whisker deprivation reorganizes serotonergic gene co-expression networks. **Mutual-information networks of** SSP genes were constructed with NETSCOPE[51], resulting in 92 highly expressed genes in L2/3 and 62 in L4, and compared across conditions by centrality differential analysis. Gene functional classes are color-coded; node size indicates betweenness centrality, normalized to total betweenness centrality. Bars above and below each network show the distribution of degree centrality and betweenness centrality across functional classes. Insets: schematic of the deprived C column and first- and second-order spared columns.

Serotonergic and dopaminergic networks are co-regulated

We next examined whether whisker deprivation coordinately regulates genes shared by the SSP and the DSP[19]. Of 20 shared genes (18 in L2/3; 10 in L4; 8 common to both), whisker deprivation produced layer-specific and coupled changes in network centrality (Fig. 7). In L2/3, *Spr* (sepiapterin reductase, which synthesizes tetrahydrobiopterin, the cofactor of the rate-

limiting enzymes of 5-HT and dopamine synthesis) and *Snca* (α-synuclein, which regulates monoamine release and transporter trafficking) exhibited the greatest increases in degree centrality across both networks, while *Maoa* (monoamine oxidase A, which degrades 5-HT and dopamine) and *Dtnbp1* (dystrobrevin-binding protein 1, which modulates dopamine and 5-HT release) showed the largest decreases (Fig. 7A,B). Betweenness centrality changes showed a broadly similar pattern, with *Snca*, *Spr* and *Gnai3* (Gαi3, which couples 5-HT1 and D2-like receptors to adenylyl cyclase inhibition) increasing and *Maoa* decreasing in both networks (Fig. 7C,D; Supplementary Fig. 3). In L4, *Pde1b* (Ca^{2+}/calmodulin-dependent phosphodiesterase 1B) increased selectively in SSP centrality with minimal effect on the DSP, while *Htr2a* (5-HT2A receptor) showed the most pronounced decrease in DSP centrality alongside a reduction in SSP centrality. *Gnaq* (Gαq, which couples 5-HT2 receptors to phospholipase C) showed opposing changes, decreasing in DSP but increasing in SSP centrality. Experience-dependent plasticity thus coordinately reorganizes serotonergic and dopaminergic molecular networks in a layer-specific manner.

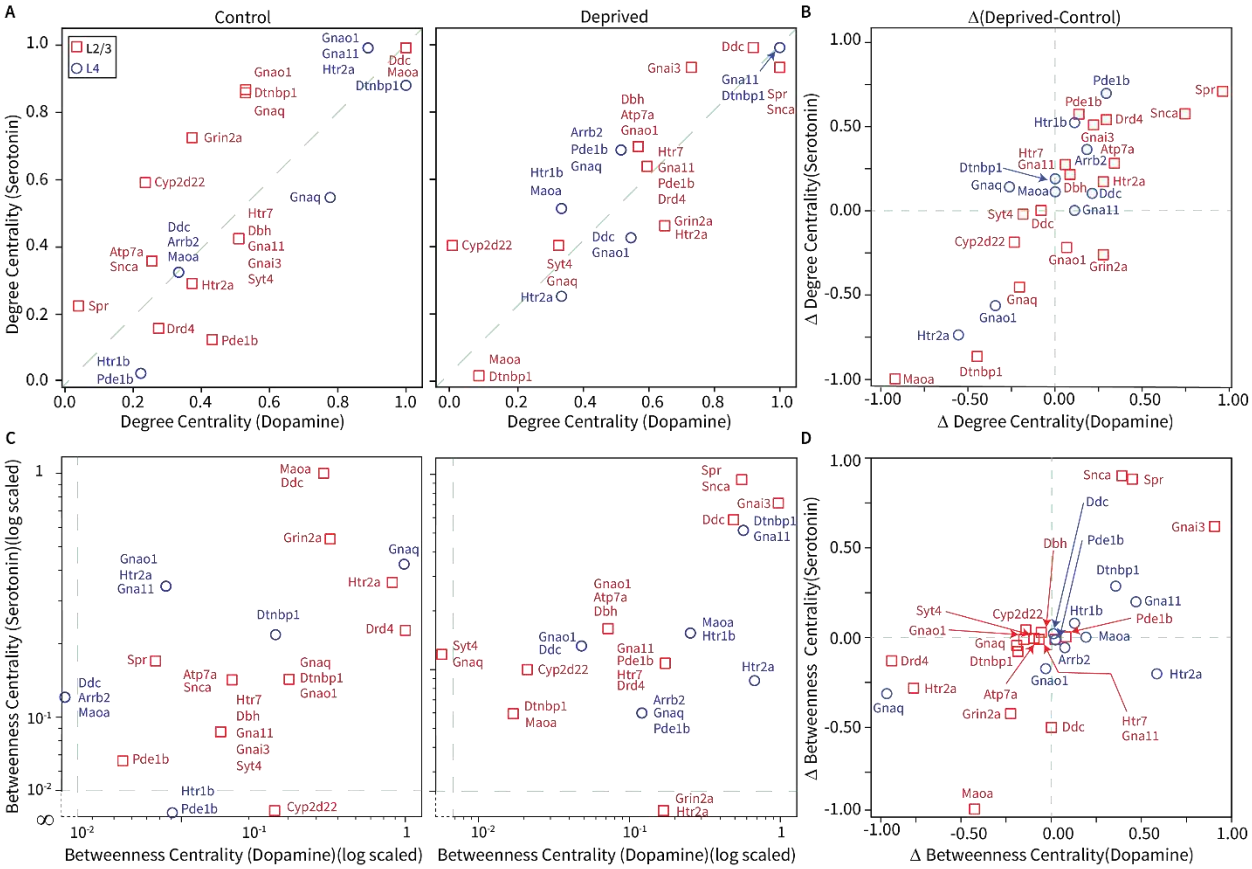


Figure 7: Shared genes of the serotonergic and dopaminergic signaling pathways are co-regulated. Twenty genes are shared between the SSP and DSP networks; eight are present in both L2/3 (squares) and L4 (circles).

A. Normalized degree centrality of shared genes in the DSP (x axis) and SSP (y axis) networks under control (left) and deprived (right) conditions.

B. Change in degree centrality (deprived − control) in the DSP and SSP networks.

C. Betweenness centrality in the DSP and SSP networks, log-scaled for visibility of individual genes; values of 0 are shown at ∞ on truncated axes.

D. Change in betweenness centrality (deprived − control) without log transformation.

DISCUSSION

This study shows that sensory experience regulates serotonergic signaling in the primary somatosensory cortex. Using laminar-resolution transcriptomics, we show that two weeks of

whisker deprivation suppresses the expression of genes governing serotonin metabolism, reuptake and release in a cortical layer- and column-specific manner. Information-theoretic network analysis reveals that these changes extend to the co-expression architecture of the serotonergic signaling pathway, with layer-specific hub genes, several of them shared with the dopaminergic pathway, emerging as candidate regulators of experience-dependent plasticity. Pharmacological activation of 5-HT1F, a receptor whose gene is differentially transcribed across the deprived barrel field, reduces L2/3 pyramidal neuron excitability. Together, these findings suggest a regulatory closed loop between sensory experience and serotonergic neuromodulation.

The layer-specificity of experience-dependent transcriptional regulation is notable. In the deprived column, changes are concentrated in L2/3, with only two transcripts (*Htr1b*, *Oaz3*) selectively regulated in L4. This contrasts with the laminar-nonspecific pattern observed in second-order spared columns (A/E), where serotonin receptor transcription is upregulated across layers. This topographic and laminar organization mirrors the specificity of adult DRN projections, which are region-, layer- and even cell-type-specific[20–22], even though serotonergic innervation of the developing cortex appears initially diffuse[47]. Our data raise the possibility that sensory experience contributes to organizing this specificity.

The finding that first-order neighboring columns (B/D) show transcriptional profiles indistinguishable from the deprived C column, despite receiving intact sensory input, is unexpected and mechanistically informative. It implies that ascending sensory drive from spared whiskers is insufficient to locally counteract deprivation-induced serotonergic dysregulation, and suggests that the neuromodulatory influence of the DRN is not simply a passive readout of local activity. The upregulation of serotonin receptor transcripts in second-order spared columns may

represent a homeostatic response that limits runaway excitation at the borders of the deprived zone, consistent with known homeostatic plasticity mechanisms in the barrel cortex[39,53–56].

The electrophysiological results link experience-dependent serotonergic transcription to neuronal function. Activation of 5-HT1F depolarized the AP threshold in L2/3 pyramidal neurons, reducing their excitability and widening the inter-spike interval, effects consistent with Gi/o-coupled inhibition of adenylyl cyclase by 5-HT1F[48]. Because the spike threshold gates how much synaptic information is transferred into spikes[57–59], and adaptation of intrinsic properties sets the working range of L2/3 neurons[60], 5-HT1F signaling is well placed to regulate information transfer in the superficial barrel cortex. These results are consistent with the broader principle that serotonin modulates the excitation–inhibition balance in sensory cortex[13,31], and with recent evidence that dopaminergic and cholinergic receptor activation reconfigures single-neuron information transfer in L2/3 in a receptor- and cell-type-specific manner[61]. They extend these principles by identifying a serotonin receptor subtype whose transcription is experience-dependent.

The parallel regulation of dopaminergic and serotonergic signaling genes by whisker deprivation, particularly of shared hub genes such as *Spr*, *Snca* and *Maoa*, points to a coordinated neuromodulatory response to altered sensory experience that extends beyond a single pathway. *Spr* supplies tetrahydrobiopterin to both tryptophan and tyrosine hydroxylases, and *Maoa* encodes monoamine oxidase A, which catabolizes both serotonin and dopamine, making both plausible points of cross-pathway integration. These findings complement our characterization of experience-dependent dopaminergic pathway regulation in the same system[19] and developmental evidence for serotonin–dopamine interactions[17,18], and suggest that sensory experience orchestrates a concerted reorganization of multiple neuromodulatory systems. Simultaneous

electrochemical detection of dopamine and serotonin[62] could test whether this transcriptional coupling is mirrored in transmitter release.

Several limitations merit consideration. First, the sample size for electrophysiology (N = 8 neurons from 4 mice) is modest, and recordings were performed in adult, non-deprived Pvalb-Cre and Sst-Cre mice rather than in the juvenile C57BL/6J mice used for transcriptomics; whether 5-HT1F activation has identical effects in the juvenile cortex, and whether these effects change after deprivation, remains to be tested. Second, at the micromolar concentration used, LY334370 may also engage other 5-HT1 receptors, and no dose–response relationship was established; selective antagonists or genetic deletion of *Htr1f* will be needed to confirm receptor specificity. Third, recorded neurons were identified visually as pyramidal; because the electrophysiological identity of cortical neurons depends on their inputs and neuromodulatory state[61,63,64], cell-type-resolved recordings will be needed. Fourth, while we demonstrate that *Htr1f* transcription is experience-dependent and that 5-HT1F activation reduces excitability, we have not shown that the transcriptional change translates to altered receptor protein levels or function in vivo; the proteome of the barrel cortex after the same deprivation protocol[65] provides a starting point. Future studies combining 5-HT biosensor imaging[25] and baseline-independent analysis of fluorescence dynamics[66] with brain-wide mapping of neuromodulatory networks[23,67] and cell-type-specific transcriptomics will be important for resolving the cellular and circuit mechanisms of this closed-loop interaction. Finally, while these results are from juvenile mice during a period of heightened plasticity, the regulatory principles identified here may inform understanding of how perturbations to serotonergic signaling, such as those caused by SSRIs or genetic variants in serotonin pathway genes, affect sensory cortex development and function[10–12].

In conclusion, these data show that sensory experience is an active regulator of the serotonergic transcriptome in the somatosensory cortex, and that serotonergic signaling in turn controls sensory neuronal excitability. This closed loop has implications for understanding how the developing brain adapts its neuromodulatory state to the sensory environment, including after sensory loss[27,28], and identifies serotonergic molecular targets for controlling cortical plasticity in health and disease.

METHODS

Ethics statement

All transcriptomic experiments were conducted in accordance with the National Institutes of Health Guidelines for the Care and Use of Laboratory Animals and were approved by the Animal Ethics Committee of Radboud University, Nijmegen, The Netherlands. Whole-cell recordings were obtained in accordance with European Directive 2010/63/EU and Dutch national regulations[49]. We have complied with all relevant ethical regulations for animal use.

Animals and sensory deprivation

Wild-type female C57BL/6J mice (Charles River, stock no. 000664) were used for transcriptomics. Animals (N = 8; 4 per group) were randomly assigned to control or whisker-deprivation groups at postnatal day 12 (P12). C-row whiskers were plucked bilaterally under isoflurane anesthesia at P12 and re-plucked as necessary until sacrifice at P23–P24[46,68]. Control animals underwent sham plucking under identical anesthetic conditions. Deprivation onset at P12 was chosen because it follows the 5-HT-sensitive developmental period (P2–P11)[69] and the transient expression of SERT in thalamocortical afferents[4,9], and coincides with the onset of active whisking[16,70]. Deprivation-induced changes therefore reflect experience-dependent plasticity rather than perturbation of serotonin-dependent barrel formation. Whole-cell recordings (N = 8 neurons from 4 adult mice) were obtained from Pvalb-Cre (RRID:MGI:5315557; 2 mice, 5 neurons) and Sst-Cre (RRID:IMSR_JAX:013044; 2 mice, 3 neurons) mice on a C57BL/6J background[49]. All animals were female.

Tissue preparation for transcriptomics

At P23–P24, mice were anesthetized with isoflurane and perfused with ice-cold carbonated slicing medium containing (in mM): 108 choline chloride, 3 KCl, 26 $NaHCO_3$, 1.25 NaH_2PO_4, 25 glucose, 1 $CaCl_2$, 6 $MgSO_4$ and 3 sodium pyruvate. Acute thalamocortical slices (400 µm) were prepared[35,37,71] and incubated in carbonated artificial cerebrospinal fluid (ACSF; in mM: 120 NaCl, 3.5 KCl, 10 glucose, 2.5 $CaCl_2$, 1.3 $MgSO_4$, 25 $NaHCO_3$, 1.25 NaH_2PO_4) at 37 °C for 30 min before gradual return to room temperature. All chemicals were purchased from Sigma-Aldrich. Cortical columns A–E were excised, and granular (L4) and supragranular (L2/3) layers were isolated under continuous ACSF perfusion at room temperature[71]. Samples from columns B/D (first-order spared) and A/E (second-order spared) were pooled within animals, yielding 8 tissue clusters across two groups. Samples were snap-frozen in liquid nitrogen and stored at −80 °C until use. All tools contacting brain tissue were treated with RNaseZap (Thermo Fisher Scientific, #AM9780).

RNA isolation and quality control

Tissue was dissolved in QIAzol (Qiagen, #79306) and RNA was isolated using the miRNeasy Mini kit (Qiagen, #217004), followed by DNase treatment (Thermo Fisher Scientific, #EN0521) and cleanup with the RNeasy MinElute kit (Qiagen, #74204). RNA integrity numbers (RIN) were determined with an Agilent TapeStation (High Sensitivity RNA ScreenTape, #5067-5581); all samples had RIN > 7.1 (range: 7.1–8.8). cDNA quality was verified by RT-PCR with *CaMKII* exon-spanning primers (FW: TCCAACATTGTACGCCTCCAT; RV: TGTTGGTGCTGTCGGAAGAT) using SuperScript II Reverse Transcriptase (Thermo Fisher Scientific, #18064014) and JumpStart ReadyMix (Sigma-Aldrich, P2893). A fragment of the expected size was amplified from all samples.

RNA sequencing

Sequencing was performed at the EMBL Genomics Core Facility (Heidelberg, Germany; RRID:SCR_004473)[46]. cDNA libraries were generated using the NEBNext Ultra RNA Library Preparation Kit for Illumina (NEB, #E7530) with oligo-dT mRNA selection and 13–14 PCR enrichment cycles. Libraries were sequenced on an Illumina NextSeq 500 (RRID:SCR_014983) in 75-bp paired-end mode using high-output flow cells. Base quality (Phred) scores ranged from 34.80 to 35.15 (>99.9% accuracy). Reads were aligned to the mm10 genome with STAR (RRID:SCR_005622), yielding 39–59 million uniquely mapped reads per sample.

Gene expression analysis

The 157 genes constituting the SSP were curated from Mouse Genome Informatics (www.informatics.jax.org) and AmiGO (amigo.geneontology.org). Differential transcription was quantified from raw counts using custom MATLAB routines. Hierarchical clustering was performed with the MATLAB clustergram function using Euclidean distances after within-lamina normalization across deprivation conditions. Laminar transcription profiles of a subset of genes were compared with in situ hybridization data from the Allen Mouse Brain Atlas (Supplementary Fig. 1).

Gene network analysis

To characterize experience-dependent changes in serotonergic gene co-expression networks, we used NETSCOPE[51], an information-theory-based toolbox for network construction from RNA-seq data. Transcript counts for the 157 SSP genes were filtered by expression level, retaining 69 genes in L2/3 and 46 in L4. Mutual information (MI) matrices were computed separately for each layer under control and deprived conditions; rows and columns with all-zero values were removed and matrices were thresholded at the mean + s.d. of the transcription rate. Degree

centrality (sum of edge weights) and betweenness centrality (node importance based on shortest-path frequency) were calculated for each gene. Between-condition differences were assessed by edge differential network analysis (Supplementary Fig. 2). The likelihood of subcellular localization of each gene (GeneCards confidence scores, 0–5) is shown in Supplementary Fig. 4.

Comparison of dopaminergic and serotonergic networks

To assess the co-regulation of the DSP and SSP by whisker deprivation, we identified genes shared between both pathways using DSP gene lists from our previous work[19]. This yielded 20 unique shared genes (18 in L2/3; 10 in L4; 8 present in both layers). Because DSP and SSP networks differ in size, normalized degree and betweenness centrality values were compared. Betweenness centrality axes were log-transformed for visualization; values of 0 are indicated as ∞ on affected axes (Fig. 7). Untransformed values are provided in Supplementary Fig. 3.

Slice preparation for electrophysiology

Adult mice were anesthetized with isoflurane and perfused intracardially with ice-cold slicing medium (composition as above)[49,72]. The brain was rapidly extracted, and coronal sections (300 µm) of the primary somatosensory cortex were cut in the same ice-cold solution, transferred to ACSF (as above) at 37 °C for 30 min and equilibrated to room temperature, aerated throughout with 95% O_2/5% CO_2.

Whole-cell recordings

Patch electrodes were pulled from borosilicate glass (outer diameter 1.0 mm, inner diameter 0.5 mm, 75 mm length; Harvard Apparatus GC100FS-7.5) with a P-2000 puller (Sutter Instrument) to resistances of 5–10 MΩ and filled with intracellular solution containing (in mM): 130 K-gluconate, 5 KCl, 1.5 $MgCl_2$, 0.4 Na_3GTP, 4 Na_2ATP, 10 HEPES, 10 Na-phosphocreatine and

0.6 EGTA (pH 7.22 with KOH). L2/3 pyramidal neurons in the barrel cortex were visually identified and patched under 40× magnification at room temperature using an EPC10 amplifier and PatchMaster v2.90.2 software. Signals were bandpass filtered (0.1–3000 Hz) and digitized at 20 kHz. Membrane potential was held at −70 mV by DC injection. Current steps (500 ms duration, 40 pA increments, 10 steps, 6.5 s inter-sweep interval) were delivered under control (ACSF) conditions and then repeated in the presence of 5 μM LY334370 (Sigma-Aldrich, SML0010) dissolved in ACSF. No dose–response experiments were performed. Neurons with resting membrane potential drift >7 mV were excluded. These recordings are part of a published database of neuromodulatory action in the adult barrel cortex[49], which has also been used to quantify dopaminergic and cholinergic regulation of single-neuron information transfer[61].

Electrophysiological data analysis

APs were detected offline in MATLAB using the findpeaks function; events with amplitude <50 mV were excluded. Firing rate was calculated as the total AP count during each depolarization step. AP threshold was defined as the peak of the second derivative of the membrane voltage[57]. The spiking time window was the interval between the first and last AP in each trial.

Statistics and reproducibility

Transcriptomic comparisons were made between N = 4 control and N = 4 deprived mice. Distributions were compared with the two-sample Kolmogorov–Smirnov test, group means with one-way ANOVA, and gene-wise or within-animal comparisons with paired t-tests, as specified in the figure legends. All tests were two-sided, and P values were corrected for multiple comparisons with the Storey false discovery rate method[73]. Electrophysiological comparisons between ACSF and LY334370 used two-sided paired t-tests within neurons (N = 8 neurons from

4 mice). Sample sizes were not predetermined by a statistical method but are similar to those of previous studies[19,46].

Data availability

RNA-seq data, including read alignments and raw read counts, are available from GigaDB[74] and can be browsed at barrelomics.science.ru.nl. Whole-cell recordings are available as part of a published database[49]. Source data underlying the graphs in the main figures are provided as Supplementary Data 1.

Code availability

NETSCOPE is openly available[51]. Custom MATLAB routines used for differential expression and electrophysiological analyses are available from the corresponding author on reasonable request.

REFERENCES

1. Daw, N. D., Kakade, S. & Dayan, P. Opponent interactions between serotonin and dopamine. *Neural Netw.* **15**, 603–616 (2002).

2. Homberg, J. R. Serotonin and decision making processes. *Neurosci. Biobehav. Rev.* **36**, 218–236 (2012).

3. Deakin, J. F. W. & Graeff, F. G. 5-HT and mechanisms of defence. *J. Psychopharmacol.* **5**, 305–315 (1991).

4. Gaspar, P., Cases, O. & Maroteaux, L. The developmental role of serotonin: news from mouse molecular genetics. *Nat. Rev. Neurosci.* **4**, 1002–1012 (2003).

5. Zhou, F. C., Sari, Y. & Zhang, J. K. Expression of serotonin transporter protein in developing rat brain. *Dev. Brain Res.* **119**, 33–45 (2000).

6. Soiza-Reilly, M. et al. SSRIs target prefrontal to raphe circuits during development modulating synaptic connectivity and emotional behavior. *Mol. Psychiatry* **24**, 726–745 (2019).

7. Laurent, A. et al. Activity-dependent presynaptic effect of serotonin 1B receptors on the somatosensory thalamocortical transmission in neonatal mice. *J. Neurosci.* **22**, 886–900 (2002).

8. Chen, X., Petit, E. I., Dobrenis, K. & Sze, J. Y. Spatiotemporal SERT expression in cortical map development. *Neurochem. Int.* **98**, 129–137 (2016).

9. Teissier, A., Soiza-Reilly, M. & Gaspar, P. Refining the role of 5-HT in postnatal development of brain circuits. *Front. Cell. Neurosci.* **11**, 139 (2017).

10. Homberg, J. R., Schubert, D. & Gaspar, P. New perspectives on the neurodevelopmental effects of SSRIs. *Trends Pharmacol. Sci.* **31**, 60–65 (2010).

11. Lee, L. J. Neonatal fluoxetine exposure affects the neuronal structure in the somatosensory cortex and somatosensory-related behaviors in adolescent rats. *Neurotox. Res.* **15**, 212–223 (2009).

12. Kroeze, Y. et al. Perinatal reduction of functional serotonin transporters results in developmental delay. *Neuropharmacology* **109**, 96–111 (2016).

13. Miceli, S. et al. Reduced inhibition within layer IV of Sert knockout rat barrel cortex is associated with faster sensory integration. *Cereb. Cortex* **27**, 933–949 (2017).

14. Pang, R. D. et al. Mapping functional brain activation using [14C]-iodoantipyrine in male serotonin transporter knockout mice. *PLoS ONE* **6**, e23869 (2011).

15. Azarfar, A. et al. An open-source high-speed infrared videography database to study the principles of active sensing in freely navigating rodents. *GigaScience* **7**, giy134 (2018).

16. Azarfar, A. et al. Serotonergic development of active sensing. Preprint at https://doi.org/10.1101/762534 (2019).

17. Schubert, D., Nadif Kasri, N., Celikel, T. & Homberg, J. R. in *Sensorimotor Integration in the Whisker System* (eds Krieger, P. & Groh, A.) 243–274 (Springer, 2015).

18. Garcia, L. P. et al. Perturbed developmental serotonin signaling affects prefrontal catecholaminergic innervation and cortical integrity. *Mol. Neurobiol.* **56**, 1405–1420 (2019).

19. Jamal, T., Yan, X., da Silva Lantyer, A., ter Horst, J. G. & Celikel, T. Experience-dependent regulation of dopaminergic signaling in the somatosensory cortex. *Prog. Neurobiol.* **239**, 102630 (2024).

20. Waterhouse, B. D., Mihailoff, G. A., Baack, J. C. & Woodward, D. J. Topographical distribution of dorsal and median raphe neurons projecting to motor, sensorimotor, and visual cortical areas in the rat. *J. Comp. Neurol.* **249**, 460–476 (1986).

21. Lee, S. B., Lee, H. S. & Waterhouse, B. D. The collateral projection from the dorsal raphe nucleus to whisker-related, trigeminal sensory and facial motor systems in the rat. *Brain Res.* **1214**, 11–22 (2008).

22. Muzerelle, A., Scotto-Lomassese, S., Bernard, J. F., Soiza-Reilly, M. & Gaspar, P. Conditional anterograde tracing reveals distinct targeting of individual serotonin cell

groups (B5-B9) to the forebrain and brainstem. *Brain Struct. Funct.* **221**, 535–561 (2016).

23. Rault, N. et al. Where top-down meets bottom-up: cell-type specific connectivity map of the whisker system. *Neuroinformatics* **22**, 251–268 (2024).

24. Sheikhkanloui-Milan, H. et al. Effects of electrical stimulation of dorsal raphe nucleus on neuronal response properties of barrel cortex layer IV neurons following long-term sensory deprivation. *Neurosci. Bull.* **26**, 388–394 (2010).

25. Ocana-Santero, G., Packer, A. M., Sharp, T. & Butt, S. J. B. Two-photon microscopy reveals sensory-evoked serotonin (5-HT) release in adult mammalian neocortex. *ACS Chem. Neurosci.* **15**, 456–461 (2024).

26. Lai, H., Makous, W. L., Quock, R. M. & Horita, A. Visual deprivation affects serotonin levels in the visual system. *J. Neurochem.* **30**, 1187–1189 (1978).

27. Jitsuki, S. et al. Serotonin mediates cross-modal reorganization of cortical circuits. *Neuron* **69**, 780–792 (2011).

28. Park, W. J. & Celikel, T. Binding as an enabling mechanism for cross-modal plasticity. *Neurosci. Biobehav. Rev.* **186**, 106695 (2026).

29. Van der Loos, H. & Woolsey, T. A. Somatosensory cortex: structural alterations following early injury to sense organs. *Science* **179**, 395–398 (1973).

30. Feldmeyer, D. et al. Barrel cortex function. *Prog. Neurobiol.* **103**, 3–27 (2013).

31. Schubert, D., Kötter, R. & Staiger, J. F. Mapping functional connectivity in barrel-related columns reveals layer- and cell type-specific microcircuits. *Brain Struct. Funct.* **212**, 107–119 (2007).

581 32. Inan, M. & Crair, M. C. Development of cortical maps: perspectives from the barrel cortex.
582 *Neuroscientist* **13**, 49–61 (2007).
583 33. Yang, J. W. et al. Development of the whisker-to-barrel cortex system. *Curr. Opin.*
584 *Neurobiol.* **53**, 29–34 (2018).
585 34. Kole, K., Scheenen, W., Tiesinga, P. & Celikel, T. Cellular diversity of the somatosensory
586 cortical map plasticity. *Neurosci. Biobehav. Rev.* **84**, 100–115 (2018).
587 35. Celikel, T., Szostak, V. A. & Feldman, D. E. Modulation of spike timing by sensory
588 deprivation during induction of cortical map plasticity. *Nat. Neurosci.* **7**, 534–541 (2004).
589 36. Clem, R. L., Celikel, T. & Barth, A. L. Ongoing in vivo experience triggers synaptic
590 metaplasticity in the neocortex. *Science* **319**, 101–104 (2008).
591 37. Allen, C. B., Celikel, T. & Feldman, D. E. Long-term depression induced by sensory
592 deprivation during cortical map plasticity in vivo. *Nat. Neurosci.* **6**, 291–299 (2003).
593 38. Foeller, E., Celikel, T. & Feldman, D. E. Inhibitory sharpening of receptive fields contributes
594 to whisker map plasticity in rat somatosensory cortex. *J. Neurophysiol.* **94**, 4387–4400
595 (2005).
596 39. Gainey, M. A. & Feldman, D. E. Multiple shared mechanisms for homeostatic plasticity in
597 rodent somatosensory and visual cortex. *Phil. Trans. R. Soc. B* **372**, 20160157 (2017).
598 40. Martens, M. B., Celikel, T. & Tiesinga, P. H. A developmental switch for Hebbian plasticity.
599 *PLoS Comput. Biol.* **11**, e1004386 (2015).
600 41. Simons, D. J. & Land, P. W. Early experience of tactile stimulation influences organization
601 of somatic sensory cortex. *Nature* **326**, 694–697 (1987).

602 42. Wimmer, V. C., Broser, P. J., Kuner, T. & Bruno, R. M. Experience-induced plasticity of
603 thalamocortical axons in both juveniles and adults. *J. Comp. Neurol.* **518**, 4629–4648
604 (2010).

605 43. Margolis, D. J. et al. Reorganization of cortical population activity imaged throughout long-
606 term sensory deprivation. *Nat. Neurosci.* **15**, 1539–1546 (2012).

607 44. Zembrzycki, A., Chou, S. J., Ashery-Padan, R., Stoykova, A. & O'Leary, D. D. Sensory
608 cortex limits cortical maps and drives top-down plasticity in thalamocortical circuits. *Nat.*
609 *Neurosci.* **16**, 1060–1067 (2013).

610 45. Simons, D. J., Carvell, G. E. & Kyriazi, H. T. Alterations in functional thalamocortical
611 connectivity following neonatal whisker trimming with adult regrowth. *J. Neurophysiol.*
612 **114**, 1912–1922 (2015).

613 46. Kole, K. et al. Transcriptional mapping of the primary somatosensory cortex upon sensory
614 deprivation. *GigaScience* **6**, 1–6 (2017).

615 47. Lidov, H. G., Grzanna, R. & Molliver, M. E. The serotonin innervation of the cerebral cortex
616 in the rat—an immunohistochemical analysis. *Neuroscience* **5**, 207–227 (1980).

617 48. Adham, N. et al. Cloning of another human serotonin receptor (5-HT1F): a fifth 5-HT1
618 receptor subtype coupled to the inhibition of adenylate cyclase. *Proc. Natl Acad. Sci.*
619 *USA* **90**, 408–412 (1993).

620 49. Yan, X. et al. A whole-cell recording database of neuromodulatory action in the adult
621 neocortex. Preprint at https://doi.org/10.1101/2022.01.12.476007 (2022).

622 50. Johnson, K. W. et al. 5-HT1F receptor agonists inhibit neurogenic dural inflammation in
623 guinea pigs. *NeuroReport* **8**, 2237–2240 (1997).

51. Bergmans, T., Jamal, T., Rezeika, A., Hsing, C.-C. & Celikel, T. NETSCOPE: information-theory based network discovery and analysis. Preprint at https://doi.org/10.1101/2022.04.18.488630 (2024).

52. Jamal, T. & Celikel, T. Evolutionarily optimized network topology as a structural prior for data-efficient sparse neural classification. Preprint at https://doi.org/10.64898/2026.03.12.711455 (2026).

53. Li, L., Gainey, M. A., Goldbeck, J. E. & Feldman, D. E. Rapid homeostasis by disinhibition during whisker map plasticity. *Proc. Natl Acad. Sci. USA* **111**, 1616–1621 (2014).

54. Gainey, M. A., Wolfe, R., Pourzia, O. & Feldman, D. E. Whisker deprivation drives two phases of inhibitory synapse weakening in layer 4 of rat somatosensory cortex. *PLoS ONE* **11**, e0148227 (2016).

55. Glazewski, S., Greenhill, S. & Fox, K. Time-course and mechanisms of homeostatic plasticity in layers 2/3 and 5 of the barrel cortex. *Phil. Trans. R. Soc. B* **372**, 20160150 (2017).

56. Greenhill, S. D., Ranson, A. & Fox, K. Hebbian and homeostatic plasticity mechanisms in regular spiking and intrinsic bursting cells of cortical layer 5. *Neuron* **88**, 539–552 (2015).

57. Huang, C., Resnik, A., Celikel, T. & Englitz, B. Adaptive spike threshold enables robust and temporally precise neuronal encoding. *PLoS Comput. Biol.* **12**, e1004984 (2016).

58. Azarfar, A., Calcini, N., Huang, C., Zeldenrust, F. & Celikel, T. Neural coding: A single neuron's perspective. *Neurosci. Biobehav. Rev.* **94**, 238–247 (2018).

59. Huang, C., Englitz, B., Reznik, A., Zeldenrust, F. & Celikel, T. Information transfer and recovery for the sense of touch. *Cereb. Cortex* **35**, bhaf073 (2025).

60. Zeldenrust, F., Calcini, N., Yan, X., Bijlsma, A. & Celikel, T. The tuning of tuning: How adaptation influences single cell information transfer. *PLoS Comput. Biol.* **20**, e1012043 (2024).

61. Joshi, N. et al. Neuromodulatory control of cortical function: cell-type-specific regulation of neuronal information transfer. *Proc. Natl Acad. Sci. USA* (in the press).

62. Khot, G., Shirtcliffe, N. & Celikel, T. Simultaneous detection of dopamine and serotonin with carbon-based electrodes. Preprint at https://doi.org/10.1101/2021.08.31.458352 (2021).

63. Joshi, N., van der Burg, S., Celikel, T. & Zeldenrust, F. Neuronal identity is not static: An input-driven perspective. *PLoS Comput. Biol.* **21**, e1013821 (2025).

64. Calcini, N., Zeldenrust, F. & Celikel, T. Electrical diversity of neurons in sensory cortices. Preprint at https://doi.org/10.1101/2024.10.07.617007 (2024).

65. Kole, K. et al. Proteomic landscape of the primary somatosensory cortex upon sensory deprivation. *GigaScience* **6**, 1–10 (2017).

66. Calcini, N., da Silva Lantyer, A., Zeldenrust, F. & Celikel, T. Nonlinear super-resolution signal processing allows intracellular tracking of calcium dynamics. *J. Neural Eng.* **21**, 036008 (2024).

67. Bergmans, T. & Celikel, T. NeuroCarta: An automated and quantitative approach to mapping cellular networks in the mouse brain. *Netw. Neurosci.* **9**, 1279–1298 (2025).

68. Celikel, T. & Sakmann, B. Sensory integration across space and in time for decision making in the somatosensory system of rodents. *Proc. Natl Acad. Sci. USA* **104**, 1395–1400 (2007).

69. Rebello, T. J. et al. Postnatal day 2 to 11 constitutes a 5-HT-sensitive period impacting adult mPFC function. *J. Neurosci.* **34**, 12379–12393 (2014).

70. Azarfar, A. & Celikel, T. Development of adaptive motor control for tactile navigation. Preprint at https://doi.org/10.1101/762443 (2019).

71. Kole, K. & Celikel, T. Neocortical microdissection at columnar and laminar resolution for molecular interrogation. *Curr. Protoc. Neurosci.* **86**, e55 (2019).

72. da Silva Lantyer, A. et al. A databank for intracellular electrophysiological mapping of the adult somatosensory cortex. *GigaScience* **7**, giy147 (2018).

73. Storey, J. D. A direct approach to false discovery rates. *J. R. Stat. Soc. B* **64**, 479–498 (2002).

74. Kole, K. et al. Supporting data for "Transcriptional mapping of the primary somatosensory cortex upon sensory deprivation". *GigaScience Database* https://doi.org/10.5524/100296 (2017).

ACKNOWLEDGEMENTS

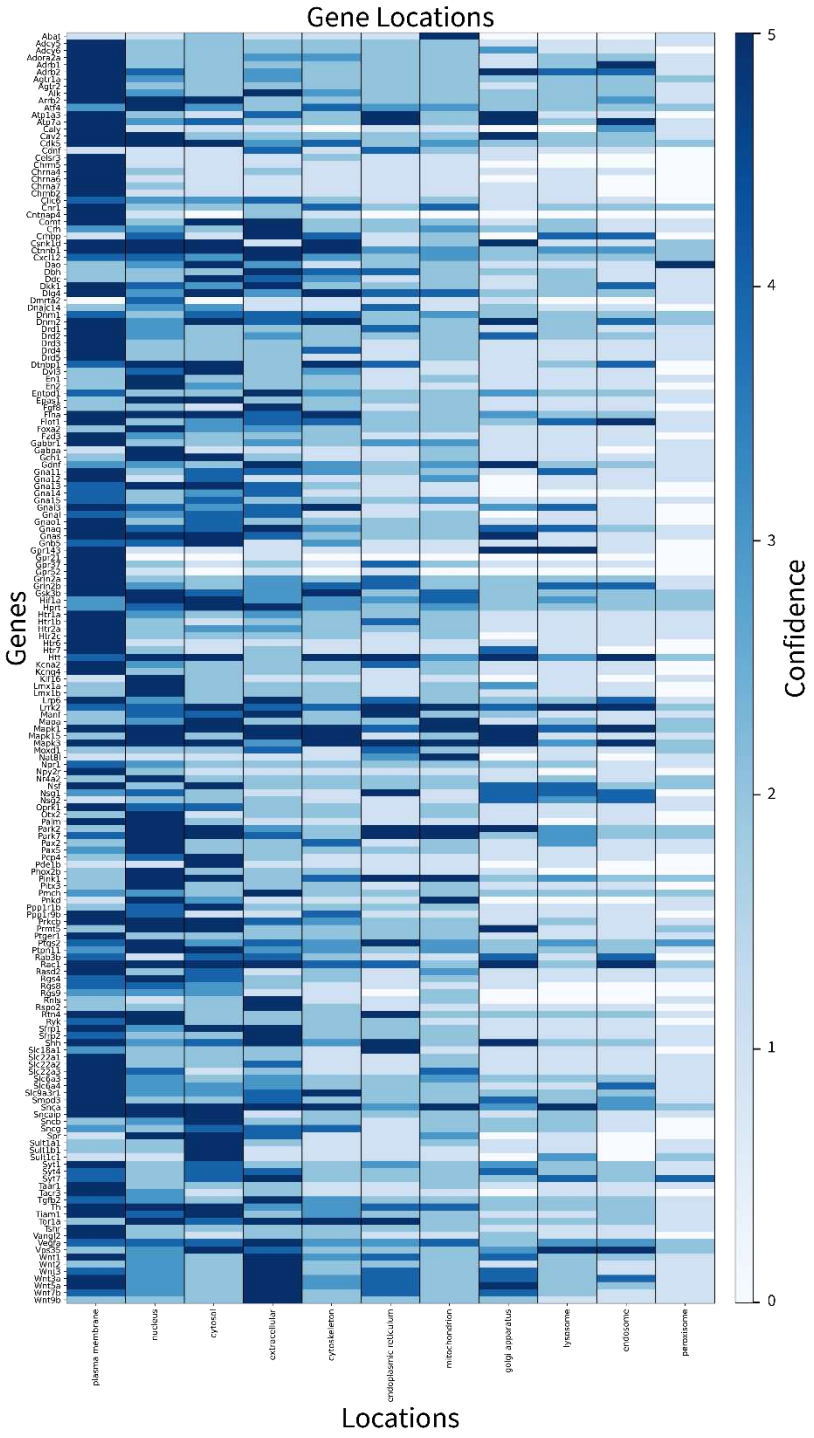
We thank members of the Department of Neurophysiology for stimulating discussions and critical feedback on the manuscript. This work was supported by grants from the European Commission (Horizon 2020, no. 860949), the European Regional Development Fund (MIND, no. 122035), and the Netherlands Organisation for Scientific Research (NWO-ALW Open Competition, no. 824.14.022) to T.C.

AUTHOR CONTRIBUTIONS

T.J. and T.C. conceived the study. T.J. performed the transcriptomic and network analyses. X.Y. performed the electrophysiological recordings. M.A.D. and Z.Z. contributed to data analysis. K.B. and J.R.H. contributed to the design and interpretation of the serotonergic and dopaminergic analyses. T.J. and T.C. wrote the manuscript with input from all authors.

COMPETING INTERESTS

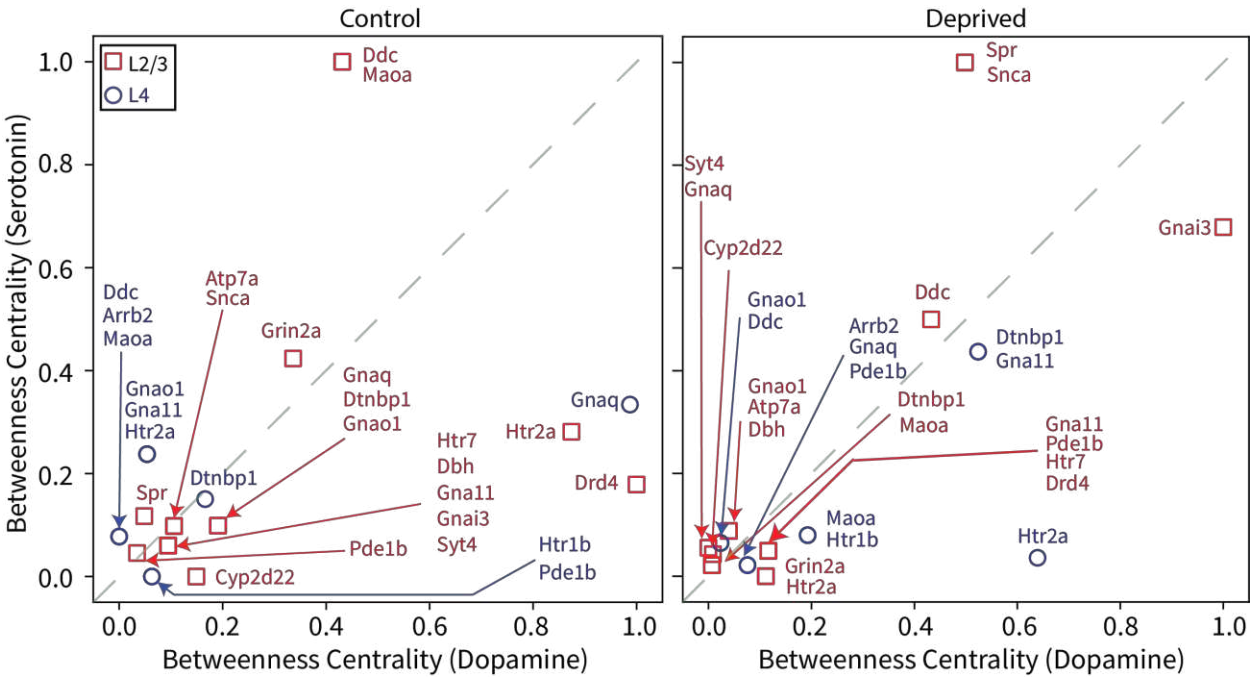
The authors declare no competing interests.



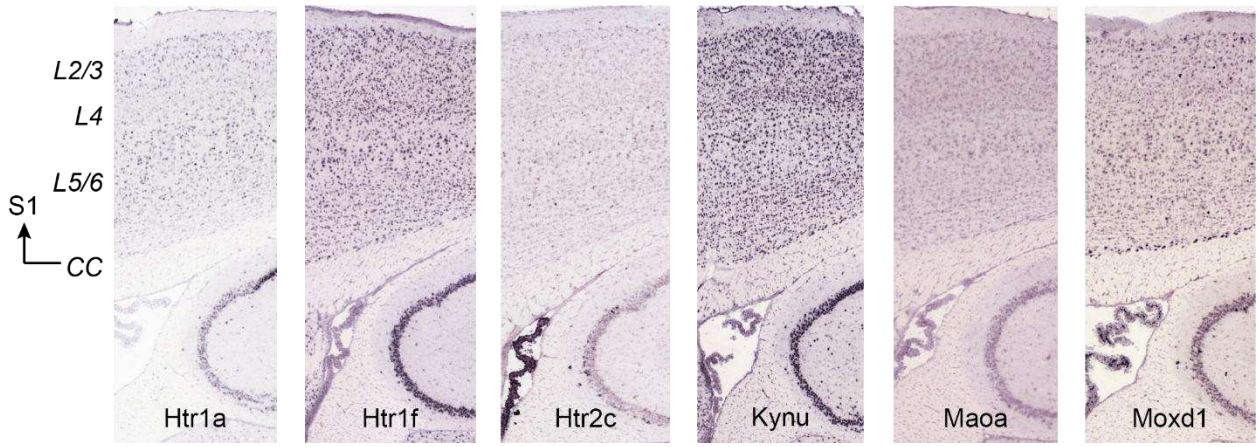
695

696

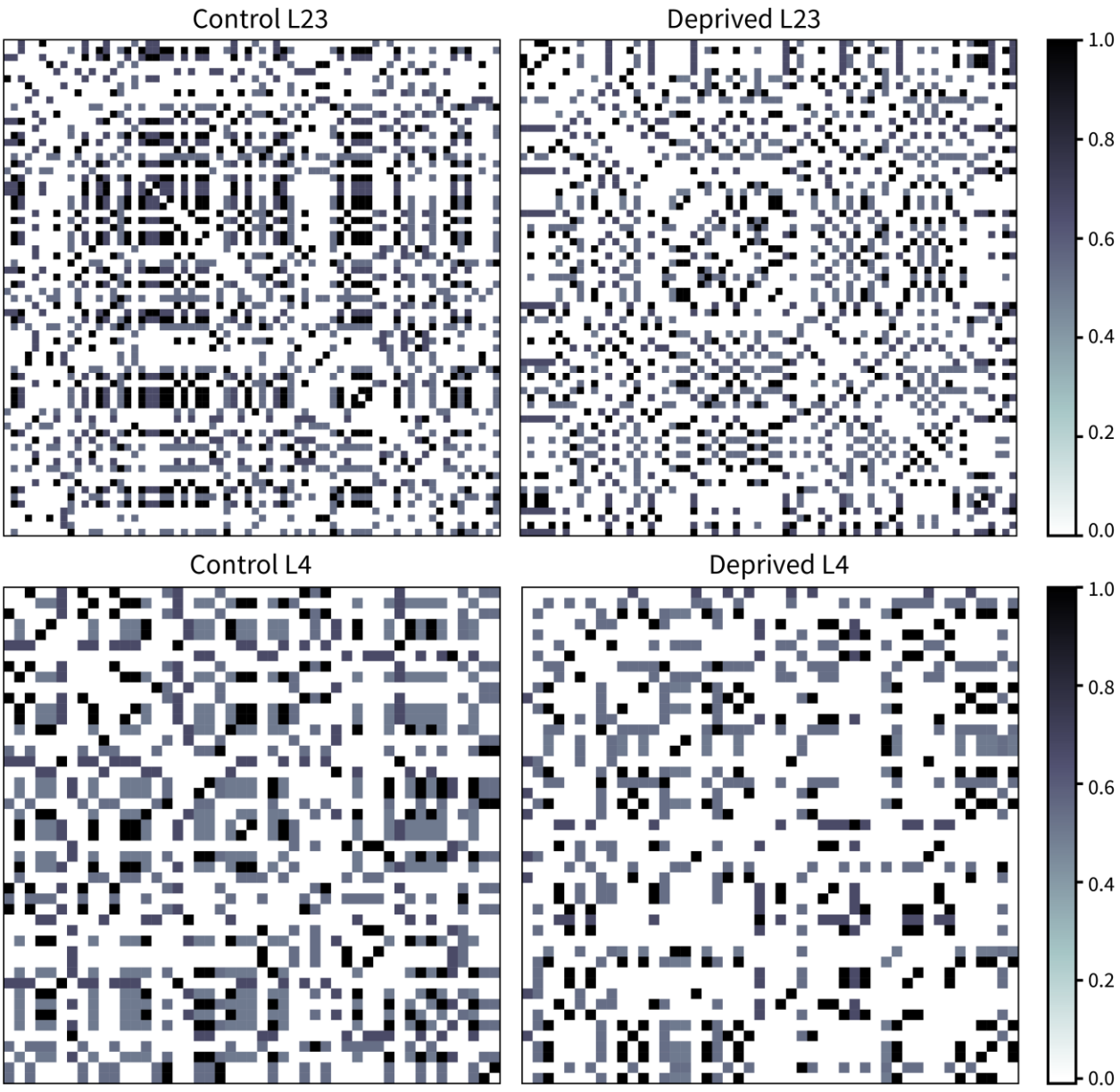
697 **Supplementary Figure 4: Likelihood of the subcellular localization of genes.** Gene
698 localization confidence levels were obtained manually from GeneCards (genecards.org), with
699 confidence scores ranging from 0 (lowest) to 5 (highest).
700



Supplementary Figure 3: Betweenness centrality of shared SSP and DSP genes in control and deprived columns in both layers, using normalized betweenness centrality values.



Supplementary Figure 1: Representative transcriptional profiles across the layers of the somatosensory cortex for a subset of genes. In situ hybridization data from the Allen Mouse Brain Atlas.



Supplementary Figure 2: Edge differential analysis of serotonergic signaling genes in control and deprived conditions. The matrices show the edge differential analysis between networks of serotonergic signaling genes under control and deprived conditions. Values are directional changes in mutual information (MI) associated with each edge. Negative values indicate edges with higher MI in the deprived group, suggesting increased interdependence among these genes after deprivation; positive values indicate edges with higher MI in the control group.